Mon. Not. R. Astron. Soc. **324**, 859–876 (2001)

A study of neutral hydrogen in five small galaxy groups

D. G. Barnes[1]★ and R. L. Webster[2]

[1]*Astrophysics and Supercomputing, Swinburne University of Technology, Mail 31, PO Box 218, Hawthorn, VIC 3122, Australia*
[2]*School of Physics, University of Melbourne, VIC 3010, Australia*

Accepted 2000 December 7. Received 2000 December 1; in original form 2000 September 19

ABSTRACT

High-resolution H I imaging observations of a heterogeneous sample of small galaxy groups are presented. The five galaxy groups studied show a broad range of individual H I properties: e.g. loose groups surrounding LGG 138 and the genuinely compact LGG 455 are identified; a massive ring of neutral gas is discovered encircling two luminous galaxies in the LGG 138 group; a galaxy-sized mass of H I is found in LGG 455 confined to an extragalactic cloud which exceeds the threshold density for star formation, yet is optically invisible; and the CCG 1 group is argued to be a chance alignment of Centaurus cluster galaxies. Global results of the study are that the deficit of H I flux in synthesis imaging data compared with single-dish data is put forward as a quantitative measure of the diffuseness of neutral gas in galaxy groups; several groups contain gas-poor galaxies that ordinarily would contain detectable quantities of H I – this is interpreted as being caused by an increased chance of gas-sweeping collisions in the group environment; and some evidence is found to support previous findings that compact groups preferentially occur in loose systems.

Key words: galaxies: evolution – galaxies: interactions – radio lines: galaxies.

1 INTRODUCTION

In this paper the results of high-resolution 21-cm neutral hydrogen observations of five small, southern galaxy groups are presented. The observations were designed to test the idea that physically loose groups of galaxies are continuously forming, and subsequently collapsing rapidly to form physically compact groups with increased elliptical fractions, or alternatively that they remain in loose configurations for tens of Gyr, in which case the compact and loose groups are drawn from separate evolutionary tracks. Five galaxy groups – LGG 138, 202 and 455, CCG 1 and HCG 91 – were studied, and a range of H I properties were found for the groups, and the individual galaxies themselves.

This paper commences with a review of compact and loose galaxy groups in Section 2, where group morphology and evolution are discussed, and a summary of previous studies of neutral hydrogen in small galaxy groups is given. In Section 3 the five small, nearby groups which are the subjects of this study are introduced. H I and broad-band optical observations and data reduction are described in Section 4, and in Section 5 the data are presented and discussed. Finally, Section 6 provides a brief discussion of the global results and some concluding remarks.

2 GALAXY GROUPS

In a reasonably complete sample of 1427 galaxies with known redshifts, within a radial distance of $25\,h_{75}^{-1}$ Mpc, Tully (1987) finds 69 per cent of the galaxies to be residing in 179 groups having two or more members. Only seven galaxies, comprising 0.5 per cent of the galaxy sample, could not be identified with higher order structure. Only 49 groups were found to have more than four members. For a larger sample of 4143 galaxies, complete to a distance of $80\,h_{75}^{-1}$ Mpc, Gourgoulhon, Chamaraux & Fouqué (1992) find 57 per cent of the galaxies to reside in 580 groups of at least two members, and 16 per cent of the galaxies to be in groups of only two galaxies. Thus most galaxies reside in groups, many of which have very few members.

2.1 Compact groups

The 'compact groups' are collections of small numbers of galaxies (i.e., 2–8 galaxies) whose projected separations are of the order of the diameters of the galaxies themselves (Rose 1977). The first manual, systematic searches for large samples of compact groups were carried out by Rose (1977) and Hickson (1982). Both searches selected compact groups on the basis of high surface density enhancements on optical survey plates, and consequently the Hickson compact groups (HCGs) are some of the (apparently) densest systems of galaxies known. Indeed, the surface densities of some HCGs are higher than those at the centres of rich clusters (Ledlow et al. 1996).

Some authors (e.g. Walke & Mamon 1989) have argued that many observed compact groups are simply chance alignments of isolated galaxies or galaxies within looser groups, i.e., the observed compact groups are *apparent* only. The main argument

★ E-mail: dbarnes@swin.edu.au

against compact groups being real physical systems is that their short crossing times imply lifetimes much shorter than the Hubble time, yet they occur in moderate numbers in the nearby Universe. However, Hickson et al. (1992) obtained redshifts for all 457 galaxies in the 100 groups, and found 92 groups to have at least three galaxies within $1000\,\mathrm{km\,s^{-1}}$ of the median velocity in the group. This is consistent with the results of Hickson & Rood (1988), which show that chance alignments of typical loose groups can account for at most 0.1 per cent of the observed compact groups. Even so, several of the Hickson groups contain members with discordant-redshifts, and Mendes de Oliveira (1995) has determined that the numbers, sizes, magnitudes and morphological types of the discordant-redshift galaxies in the Hickson compact groups are as expected if the discordant galaxies are chance projections of unrelated galaxies. Concordant velocities amongst HCG members is generally satisfactory evidence that the galaxies reside within a common structure larger than the compact group.

The width of the distribution of HCG galaxy velocities relative to the median velocity of each group is $\sim 250\,\mathrm{km\,s^{-1}}$, which is similar to loose group velocity dispersions, and significantly less than rich cluster velocity dispersions (Hickson 1997). Based on radial velocities and angular sizes, the HCGs exhibit short dynamical times on the order of 250 Myr, and a mean mass-to-light ratio of $67\,h_{75}\,\mathrm{M_\odot/L_\odot}$ (Hickson et al. 1992). Mass-to-light ratios of individual HCG galaxies are typically $9\,h_{75}$ solar units (Rubin, Ford & Hunter 1991), so the galaxies appear to contain only 15 per cent of the total mass in the groups (Hickson 1997). This is compatible with the findings of Pildis, Bregman & Evrard (1995), who determine a baryon fraction of 5–19 per cent for a small sample of HCGs having diffuse *ROSAT* X-ray detections.

2.2 Loose groups

'Loose groups' are an ill-defined subset of galaxy groups. The catalogues of Fouqué et al. (1992), Garcia (1993) and Nolthenius (1993) are all accepted as containing loose groups of galaxies, yet there is no standard definition of loose groups as there is for the compact groups (i.e., the Hickson 1982 criteria). Spatial coincidences between HCGs and loose groups have been detected recently by Rood & Struble (1994), who show that a remarkable 70 per cent of nearby observed compact groups are located within loose groups. Ramella et al. (1994) support this finding: in their HCG subsample comprising 38 groups, 29 are found in rich, looser systems. Furthermore, recent X-ray data have shown that while ~50 HCGs coincide with X-ray sources on scales up to 30 arcmin, it is only in ~15 of these groups that the X-rays are likely to originate from the compact group itself (Ebeling, Voges & Böringer 1994). This would be expected if many of the HCGs were not isolated, but rather were embedded in larger, looser groups or clusters containing a hot, diffuse gas. Numerical simulations of compact group formation by Pildis, Evrard & Bregman (1996) support this hypothesis, in the sense that X-ray-luminous, diffuse gas is seen in substantial quantities well before the forming group becomes compact. Ponman & Bertram (1993) present X-ray evidence supporting this finding for the case of HCG 62, where the compact core of galaxies is believed to have formed recently within a looser group, and will probably merge to form a single elliptical remnant within 1 Gyr. Given that the lifetime of compact groups is short, loose groups and poor clusters must be ideal, indeed favourable, environments for the formation of compact groups. Thus loose groups are an important class of groups to study alongside compact groups.

2.3 Neutral gas in small groups

The distribution and kinematics of neutral gas in galaxy groups can be studied using 21-cm emission-line observations of neutral hydrogen (H I). In particular, since H I is an extended disc tracer in normal galaxies, high-resolution H I observations can be used to search for evidence of galaxy interactions within groups. Groups for which H I maps indicate recent interaction history, i.e., exhibit features such as tidal tails, bridges or debris, are likely to be true physical systems. Measured deficiencies in the total H I mass of individual galaxies within groups are also interesting, because the 'missing' gas must either become ionized at some stage during the formation and evolution of the group, or must be dispersed over a large volume, making detection more difficult. Alternatively, perhaps the star-forming history differs significantly in compact group galaxies – there is now evidence that tidal interactions and mergers, such as are commonly seen in the HCGs, are star formation triggers. Sanders & Mirabel (1996) report that the trigger for intense infrared emission from luminous infrared galaxies in the nearby Universe appears to be the strong interaction and merger of spiral galaxies that are rich in molecular gas. If this is the case, then star formation may be accelerated in compact group galaxies, thus depleting neutral gas more rapidly than for otherwise similar field galaxies.

Williams & Rood (1987) observed half of the HCGs in the 21-cm line of neutral hydrogen using single-dish telescopes, and detected integrated H I profiles for two-thirds of the groups. They find that, on average, an HCG contains half as much neutral hydrogen as a loose group with similar constituent galaxies. This again suggests that the compact groups are real, since such an effect would not be seen if compact groups were in fact projected configurations of loose groups. Oosterloo & Iovino (1997) support this finding by re-analysing the data from Williams & Rood, using new optical images and redshift information for HCGs, and their own observations of 14 southern compact groups (SCGs) (Prandoni, Iovino & MacGillivray 1994). They find the H I deficiency in HCGs to be significant (at the 99.9 per cent level) compared to a small control sample of field spirals, and also the H I deficiency in SCGs to be significant (at the 85 per cent level).

There have only been a handful of synthesis observations of compact groups at the 21-cm wavelength. For example, Shostak, Sullivan & Allen (1984) find that in Stephan's Quintet, the bulk of the H I at all velocities lies outside the optical galaxies. Williams & van Gorkom (1988) find H I emission in a single cloud surrounding HCG 18, smoothly distributed over a region twice the optical size of the compact group. They also find that the cloud is in regular rotation with period less than 0.8 Gyr. However, recent Hα observations by Plana et al. (2000) have demonstrated that HCG 18 is probably a single irregular galaxy undergoing clumpy star formation – at least confirming that the Hickson (1982) selection criteria can identify veritable physical systems.

Williams, McMahon & van Gorkom (1991) have imaged three groups – HCGs 31, 79 and 44. For two of these groups they find H I clouds much larger than the galaxies, whilst for the third they find H I emission located within individual galaxies only. Koribalski (1996) has observed several tidal tails tracing possible H I connections between the galaxies in the Grus Quartet. It appears that three of the galaxies in the Quartet are embedded in a low column density H I envelope. Oosterloo & Iovino (1997) observed seven compact groups, and highlight a group which is very poor in H I but exhibits signs of tidal interaction, and also a group which is rich in H I, a large fraction of which forms a

common envelope. Based on their observations, two more of their groups exhibit interactions, whilst the other three appear to be relatively interaction-free at present.

3 A SAMPLE OF SMALL, NEARBY GROUPS

To enable a preliminary study of the H I properties of nearby compact and loose poor galaxy groups, a sample of five nearby groups has been selected for 21-cm H I imaging using the Australia Telescope Compact Array (ATCA) near Narrabri in New South Wales (NSW), Australia, and for broad-band colour imaging using the Mount Stromlo 40-inch telescope at Siding Spring Observatory near Coonabarabran in NSW. The observations were designed to provide valuable new information on the distribution, dynamics and evolution of neutral atomic hydrogen in small groups of galaxies, as well as to provide general pictures of stellar populations and formation histories within the galaxies. In particular, the five groups were chosen in the hope that they would shed light on the following questions.

(i) Can physically loose and compact groups be distinguished by the absence or presence of a large-scale halo of H I? Does an intermediate type of group exist in which a halo is in the process of forming, thereby connecting the evolutionary paths of loose and compact groups?

(ii) Are large H I shell structures, such as those reported in giant field ellipticals by Malin & Hadley (1997), seen in galaxy groups? If so, are these structures malformed large-scale H I haloes, or instead the result of violent merger processes between galaxies in a group?

(iii) Do groups have large-scale, optically invisible or very low surface brightness H I clouds associated with them? If so, are such clouds 'failed' galaxies (i.e., true intergalactic H I clouds), or are they material that has been tidally stripped from group members?

(iv) Is the observed H I deficiency of compact groups a real effect and, if so, how is the galactic H I in groups distributed differently to that in isolated gas-rich galaxies? Can a redistribution of the H I within a compact group lower the observed H I density? Can the state of the neutral gas be used to characterize the evolutionary state of the group?

(v) Do there exist intermediate-density groups in which weak but long-term tidal effects slowly displace or distort the H I relative to the stellar population in otherwise normal disc galaxies?

The groups are drawn from the catalogues of Hickson (1982) and Garcia (1995), and from Barnes & Drinkwater (1994). The five groups have varying compactness, morphologies, sizes and redshifts, and are listed in Table 1. Column 4 gives the radial velocity of each group in $\mathrm{km\,s^{-1}}$: this is the median galaxy heliocentric velocity for the HCGs (from Hickson et al. 1992), the mean radial velocity for the LGGs (from Garcia 1995), and an estimate of the mean radial velocity for CCG 1 (from Barnes & Drinkwater 1994). Column 6 lists the group classification: this is the type of the group according to Hickson's (1982) classification scheme, where S (E) indicates that the brightest galaxy is a spiral (elliptical), and the qualifiers I, II and III indicate that the brightest galaxy is brighter in red magnitude than the second brightest galaxy by at least one magnitude, less than one but greater than one-half magnitude, and less than one-half magnitude respectively.

3.1 LGG 138

First recognized by Garcia (1993) as a nearby group, LGG 138 contains the five galaxies NGC 2280, 2292 and 2293, and ESO 490− G010 and G045. LGG 138 has a projected size on the sky of order 1°, rendering it invisible to previous searches which lacked redshift information. The group has a most likely three-dimensional velocity dispersion of $400\,\mathrm{km\,s^{-1}}$. LGG 138 was selected for H I imaging because it is nearby and visually interesting. The NGC 2292 and 2293 galaxies are both early-type spirals of nearly identical optical luminosities and morphologies, probably located near the dynamical centre of the group. Separated by only 0.8 arcmin, corresponding to a projected physical separation of $6.3\,h_{75}^{-1}$ kpc at a distance of $27\,h_{75}^{-1}$ Mpc, this pair of galaxies was thought to be an excellent candidate for the study of a nearby dense system, possibly exhibiting a merger event.

3.2 LGG 202

This group was identified by Garcia (1993, 1995) as comprising the three galaxies NGC 3267, 3269 and 3271. It is located nearby (and probably behind) the Antlia cluster, which is a small cluster embedded in the Hydra-Centaurus supercluster (Ferguson & Sandage 1990). The Antlia cluster has associated with it four smaller systems which are unlikely to be bound to Antlia (Hopp & Materne 1985). The situation of LGG 202 in a cluster environment, and the morphological concordance of its member galaxies (i.e., they are all early-type spirals of nearly identical magnitudes), make it an interesting target for H I-deficiency measurements.

3.3 CCG 1

This fine example of a compact group was first recognized as the

Table 1. An heterogeneous sample of small, nearby groups – see text for a description of the columns.

Name	RA (J2000)	Dec. (J2000)	Velocity ($\mathrm{km\,s^{-1}}$)	Members	Class.	Diameter (h_{75}^{-1} kpc)
(1)	(2) h m s	(3) ° ′ ″	(4)	(5)	(6)	(7)
LGG 138	06 47 37	−26 43 56	1744	4	SII	360
LGG 202	10 30 08	−35 18 28	3481	3	SII	182
CCG 1	12 40 52	−36 43 58	3400	3	SII	53
HCG 91	22 09 12	−27 46 33	7135	4	SI	144
LGG 455	22 15 42	−45 50 25	1984	3	SIII	78

AM 1238-362 triplet of galaxies by Arp & Madore (1987), and was re-identified in an automated search for compact groups in the COSMOS catalogue (Barnes & Drinkwater 1994). CCG 1 was selected for imaging because of the high density of the group and the peculiar ring-like appearance of ESO 381- G009.

3.4 HCG 91

First identified as a triplet by Vorontsov-Velyaminov (1977) in an atlas of interacting galaxies, this group was rediscovered by Hickson (1982) as a group of four galaxies. NGC 7214 shows faint Hα emission towards the east of the nucleus (Gonzalez Delgado et al. 1997), and appears to be interacting with ESO-LV 4670121 which presently lies at a projected distance of only $16\,h_{75}^{-1}$ kpc northwards. This interaction has been detected at 60 and 100 μm in reprocessed *IRAS* data (Allam et al. 1996).

3.5 LGG 455

Like CCG 1, this is another fine example of three closely associated galaxies on the sky, for which redshift information has shown velocity concordance. The group actually consists of four galaxies, three of which lie within 5 arcmin of each other, whilst the fourth is some 10 arcmin south of the triple. NGC 7232 and 7233 are a suspected interacting pair (Lauberts 1982; Corwin, de Vaucouleurs & de Vaucouleurs 1985), and are separated in velocity by less than 50 km s^{-1}. NGC 7232B appears to have distended spiral arms that have possibly been dragged out tidally by a recent close encounter. LGG 455 is ideal for H I imaging because of its low redshift, and compact nature on the sky. Since the H I in an interacting system is expected to be significantly disturbed, observations of this system will at least demonstrate its state of interaction, and may uncover neutral gas that has been tidally stripped from the galaxies.

4 OBSERVATIONS

4.1 21-cm spectral line imaging

The five groups were observed using the Australia Telescope Compact Array (ATCA) near Narrabri in New South Wales, Australia. The ATCA is described in 'The Australia Telescope', a special issue of the Journal of Electrical and Electronics Engineering Australia (1992).

4.1.1 Observations

The pointing centres and array configurations for the five groups are shown in Table 2. The half-power primary beamwidth of a single ATCA antenna at 21 cm is 33 arcmin, which is sufficient to fully image the LGG 202, CCG 1, HCG 91 and LGG 455 groups with only one pointing each. However, in the case of LGG 138, the diameter of the group is nearly 1°, and so the observations were directed at the NGC 2292/2293 pair. For all observations, the AT correlator collected dual-polarization data, and the observing bandwidth was 16 MHz with 31.25-kHz channels. The velocity resolution for this correlator configuration is 1.21 times the channel width, i.e., 8.0 km s^{-1}.

Observations with two different ATCA configurations – 750A and 1.5D – were obtained for the groups CCG 1, HCG 91 and LGG 455. Observations with five different array configurations were acquired for LGG 138, and LGG 202 was observed only with the 750A configuration. The imaging properties of the various array configurations used are shown in Table 3. The primary calibrator, used to determine the absolute flux scale as well as the bandpass calibration, was the standard ATCA flux calibrator 1934-638 (14.9 Jy at 1384 MHz; Reynolds 1994), and was observed for approximately 10 min per group. Secondary calibrators were observed for typically 5-min intervals every 30 min to determine instrumental and atmospheric phase variations.

Table 2. Pointing centres and array configurations (excluding baselines over 3000 m) for the ATCA observations of the southern groups.

Group	POINTING CENTRE RA (J2000)	Dec. (J2000)	Velocity (km s^{-1})	Array configuration/s	Baseline range (m)	Integration time (h)
	h m s	° ′ ″				
LGG 138	06 47 24	−26 44 05	1800	750A, 750B 1.5B, 1.5C, 1.5D	31–1485	47.3
LGG 202	10 29 50	−35 16 14	3517	750A	77–735	10.0
CCG 1	12 40 41	−36 42 42	3507	750A, 1.5D	77–1439	20.6
HCG 91	22 08 54	−27 47 26	7188	750A, 1.5D	77–1439	19.7
LGG 455	22 15 38	−45 50 04	1756	750A, 1.5D	77–1439	20.5

Table 3. 21-cm imaging properties of the ATCA (excluding baselines over 3000 m), and observation dates.

Array configuration	Baseline range (m)	Theoretical resolution (RA; arcsec)	Largest structure (RA; arcmin)	Observation date
750A	77–735	59	9.4	1996 November
750B	61–765	57	12	1997 August
1.5B	31–1286	34	23	1997 August
1.5C	77–1485	29	9.4	1997 September
1.5D	107–1439	30	6.7	1997 March

4.1.2 Data reduction

Editing, calibration and imaging of the visibility data were accomplished using the standard ATCA data reduction package MIRIAD. Table 2 shows the total effective integration time obtained for each group and array configuration. These times are determined from the number of complex visibilities remaining after flagging.

The MIRIAD task INVERT was used to produce channel maps from the calibrated visibility data. The two standard visibility weighting schemes were utilized for producing maps: natural and uniform weighting. Pixel sizes were selected individually for each group and weighting function pair, to obtain the recommended sampling of the beam for deconvolution. The data were averaged into velocity planes of constant width 13.2 km s^{-1} in order to improve dynamic range and minimize smearing of signals over several channels in the output image.

All maps – except those of LGG 202 which showed no detectable emission – were cleaned using CLEAN. Upto 10 000 minor iterations of a Clark CLEAN algorithm (Clark 1980) were used to clean to a depth of 1σ. Deeply cleaned images give nearly correct fluxes, since the flux remaining in the residual map is small compared to the flux represented by the clean components, and thus no rescaling (e.g. Jörsäter & van Moorsel 1995) is needed to account for the clean and dirty beams having different areas. To prevent corrugations in the cleaned images, a Cornwell Prussian Hat parameter of 0.2 was used. The resultant clean maps are essentially free of sidelobe structure from moderate to strong line sources.

4.1.3 Image statistics

Table 4 shows the root mean square (rms) flux sensitivities (1σ), in mJy per dirty beam, for the uncleaned channel maps. The clean beam shapes are also given in Table 4. The 1σ column density sensitivity is calculated under the usual assumptions that the line-emitting H I is optically thin and that the temperature of the surrounding radiation field is small compared to the spin temperature of the H I. Note that the column density sensitivity is shown for the dirty channel maps. For reference, the theoretical noise obtained in ATCA channel maps of width 13.2 km s^{-1} for a 10-h observations is 1.1 mJy beam^{-1}.

4.2 HIPASS images of the groups

The H I Parkes All Sky Survey (HIPASS – see Barnes et al. 2001) has imaged the entire southern extragalactic sky in neutral hydrogen emission. The HIPASS scans covering a $2.5° \times 2.5°$ field surrounding four of the five galaxy groups imaged at the ATCA were extracted from the archive, and gridded into position–velocity cubes to image the wider environment of each group. The HIPASS data complement the higher resolution ATCA data with wide-field imaging capabilities, and can be used to determine an upper limit to the total H I flux of an unresolved galaxy or group of galaxies. The standard robust processing and gridding parameters were used to generate the HIPASS group data cubes (Barnes et al. 2001). The rms noise in the HIPASS images were between 10.8 and 14.4 mJy beam^{-1}.

4.3 Broad- and narrow-band optical imaging

The groups were also observed using the Mount Stromlo Observatory (MSO) 40-inch telescope at Siding Spring Mountain, Coonabarabran, in NSW. Broad-band images (in the *B*, *V*, and *R* bands) were acquired. For the observations, the new Tek2K thinned charge-coupled device (CCD) was installed at the Cassegrain focus of the telescope. The CCD has 2048×2048 elements, and a pixel scale of 0.6 arcsec pixel^{-1} when mounted on the telescope. To improve sensitivity to low surface brightness features, and to decrease the CCD readout time, 3×3 CCD pixels were binned into single image pixels prior to readout, resulting in raw image files having square pixels of side length 1.8 arcsec. Most of the images were acquired in non-photometric conditions.

Dark frame subtraction, flat-fielding and basic calibration of the 40-inch images were applied using standard procedures in the optical data reduction package IRAF. Each image presented herein is the pixel-by-pixel median image of three separate frames.

4.4 Analysis

Zeroth-order moment maps of the synthesis images have been generated after applying the technique described by Barnes (1998) for selecting an appropriate smoothing kernel and threshold flux for moment analysis. The restored H I data cubes were smoothed using a spatial median filter of box size 5×5 pixels, and pixels in the unfiltered cubes were not considered in the moment calculation when the corresponding pixel in the smoothed cube was below 2.2 times the nearby rms noise level. The MIRIAD task MOMENT was used for the calculation of moments. The resultant maps, in units of Jy beam^{-1} (km s)$^{-1}$, were converted to H I column density maps under the usual assumptions. Because the maps were mostly devoid of emission outside the central 6–8 arcmin of each imaged field, no correction for the primary beam shape has been necessary.

Table 4. Image statistics for the dirty channel maps. The column density sensitivity is per 13.2 km s^{-1} plane, assuming that the H I is optically thin, and that the temperature of the surrounding radiation field is small compared to the spin temperature of the H I. The beam shape listed for LGG 202 has been determined to allow the calculation of column density limits for the group, even though a clean was not performed.

Group	NATURAL WEIGHT IMAGES			UNIFORM WEIGHT IMAGES		
	Restoring beam	RMS SENSITIVITY 1σ (mJy per dirty beam)	(10^{18} $N_{H\,I}$ cm^{-2})	Restoring beam	RMS SENSITIVITY 1σ (mJy per dirty beam)	(10^{18} $N_{H\,I}$ cm^{-2})
LGG 138	$71'' \times 34''$	0.78	4.7	$43'' \times 20''$	1.11	19
LGG 202	$87'' \times 73''$	1.88	4.3	–	–	–
CCG 1	$54'' \times 34''$	1.19	9.4	$34'' \times 22''$	1.59	31
HCG 91	$69'' \times 40''$	1.34	7.2	$45'' \times 23''$	1.88	26
LGG 455	$53'' \times 43''$	1.22	7.9	$31'' \times 26''$	1.62	29

Peak H I intensity maps were derived from the HIPASS position–velocity cubes using the MIRIAD task XPEAK. In order to enhance low surface brightness features, each cube was median-filtered spatially with a square kernel of sidelength 20 arcmin (5 pixels) prior to generating the peak-intensity map.

Central velocities and widths were determined from integrated spectra using a script which iterates twice to find the peak flux and the 50 and 20 per cent velocity points. The first iteration establishes the rough location of the source in the spectrum. Following this, a baseline is subtracted from the integrated spectrum by determining the median flux of all spectral channels *except* those identified as containing flux, and the peak flux and velocity points are redetermined using the baseline-subtracted spectrum. The central recessional velocity of a source was assigned to be the velocity halfway between the 20 per cent peak velocities. The formal (resolution-limited) uncertainties in the velocities are $16\,\mathrm{km\,s^{-1}}$ per single velocity measurement in both the HIPASS and ATCA data cubes; consequently, the formal uncertainty for quoted central velocities and widths is $23\,\mathrm{km\,s^{-1}}$.

H I positions were measured from zeroth-order moment maps, generated over the 20 per cent velocity width of each source, using the MIRIAD routine IMFIT. IMFIT finds the 'least sum of squares' Gaussian fit to the source.

Total integrated H I fluxes were derived from ATCA cubes using the histogram subtraction method described in Barnes (1998). In a few difficult cases, the integrated fluxes were measured from integrated spectra between the 20 per cent peak velocity points. Fluxes should be considered accurate to 15 per cent.

Under the usual assumptions the H I mass of a source with integrated flux S Jy km s^{-1} was determined using the standard expression $M_{\mathrm{H\,I}} = 2.356 \times 10^5 (V/75)^2\, S\, h_{75}^{-2}\, \mathrm{M}_\odot$, where V is the central radial velocity of the galaxy expressed in km s^{-1}. H I masses carry similar uncertainties to H I fluxes, increased slightly by the uncertainty in deducing distances to galaxies. Consequently, the H I masses cited are believed accurate to order 20–25 per cent. Radial velocities have been corrected for the Sun's motion with respect to the Local Group.

For galaxies where the parametrized eccentricity is available in the COSMOS/UKST Southern Sky Object Catalogue, the eccentricity has been used to apply a first-order inclination correction to the velocity widths. For a thin, circular disc, the maximum circular speed is $W_{20}/2e$, where W_{20} is the full velocity width at 20 per cent peak flux, and e is the eccentricity derived from the COSMOS parameters for the source. This correction is, of course, uncertain for nearly face-on galaxies.

H I mass-to-light ratios have been derived for unconfused galaxy detections using the H I mass determined as described above and total B and V magnitudes from Lauberts & Valentijn (1989). Corrections have been made for absorption in edge-on systems using the formula $\Delta m = 0.70 \log_{10} \sec i$ (de Vaucouleurs, Corwin & de Vaucouleurs 1976), where i is the inclination angle of the galaxy with respect to the sky, and is determined from the COSMOS eccentricity of the source. This correction is necessary, since optical absorption is significantly greater than 21-cm absorption, and consequently there is a trend towards higher apparent H I mass-to-luminosity ratios for edge-on systems. The total B and R magnitudes assigned to the Sun for these calculations are 5.48 and 4.31 respectively (Allen 1973).

4.4.1 *Group membership and parameters*

For the LGG 138 and 455 and CCG 1 groups, new members of the groups were detected in the observations. Galaxies are accepted as members of the groups if their radial velocities lie within $500\,\mathrm{km\,s^{-1}}$ of the median velocity of the group. The aim is to consider each group as a loose group, potentially with a number of members which form a dense condensation (i.e., a compact group) within the larger group. Groups to which new members were added from the results of the H I observations have 'H I' incorporated in their names, e.g., 'CCG H I 1.' The physical state of each group is parametrized with the median galaxy–galaxy displacement, the median radial velocity, and a median projected velocity dispersion. This dispersion is the median of the absolute differences between the radial velocities of all group members and the median velocity of the group. Finally, the mass estimators of Heisler, Tremaine & Bahcall (1985) are used to determine a dynamical estimate of the total group mass, assuming that all members are bound in circular orbits.

5 THE GROUPS

5.1 LGG 138

Eight galaxies were detected in H I emission in the $4° \times 4° \times 2670\,\mathrm{km\,s^{-1}}$ HIPASS cube centred on the NGC 2292/2293 pair in LGG 138 – see Fig. 1. The measured parameters of these galaxies are shown in Table 5; a description of the columns follows.

Columns (1)–(2). J2000 coordinates of the H I detection.

Columns (3)–(4). Central velocity and velocity width as determined from the 50 per cent peak flux points.

Columns (5)–(6). Central velocity and velocity width as determined from the 20 per cent peak flux points.

Columns (7). Integrated H I flux of the source. For ATCA data, this is the primary-beam-corrected H I flux as derived using the histogram subtraction method described in Barnes (1998).

Columns (8) and (14). Catalogue name and number, and offset in arcmin from the H I position: identifications are made on the basis of good agreement in position and velocity. When no velocity has been previously measured, an identification is made only where there is good agreement in position, and consistency between optical morphology and H I profile shape.

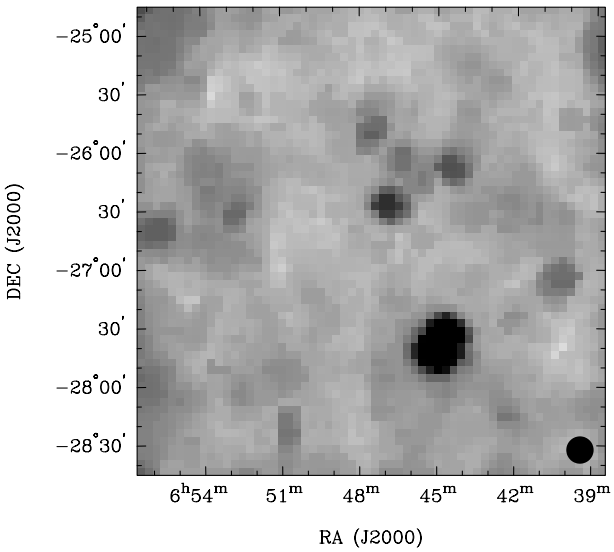

Figure 1. Peak H I intensity map of LGG 138 derived from spatially smoothed HIPASS data. The 14.4-arcmin observing beam is shown in the lower right corner.

Columns (9)–(10). Previously known heliocentric radial velocity, and uncertainty if known, and corresponding literature reference, given as an index to the bibliography listed beneath the table.

Columns (11)–(12). Total Cousins *B* and *R* magnitudes from Lauberts & Valentijn (1989), accurate to 0.1 mag.

Column (13). Eccentricity of optical counterpart, derived from the COSMOS/UKST Southern Sky Object Catalogue where possible. This is not provided for galaxies that are divided by COSMOS into several subobjects. The purpose of recording the eccentricity is to make possible an estimate of the inclination angle for later use.

Column (15). Notes:

(a). ESO 490− G046 has a star superimposed on the image, rendering magnitudes unreliable.

(b). ESO 490− G045 was detected in both the HIPASS and ATCA data. The catalogue parameters are repeated here for easy comparison.

(c). This object is identifed as a ring of neutral hydrogen surrounding the pair of (possibly) interacting or merging galaxies, NGC 2292/2293. The neutral hydrogen is associated in some way with these two galaxies, but is not detected near the nuclei of the galaxies.

(d). These galaxies were not detected in H I emission; the positions listed are optical positions. ESO 490− G010 was not detected, since it lies beyond the field of view imaged by the available HIPASS and ATCA data.

(e). These galaxies were not *directly* detected in H I emission, other than the gas ring encircling them on the sky; the positions listed are optical positions.

(f). There is some disagreement in the literature on the radial velocities of these galaxies. Those listed here have been selected for the reasons outlined below and in Section 5.1.

Two H I sources were identified in the $40 \times 40\,\mathrm{arcmin}^2 \times 1000\,\mathrm{km\,s^{-1}}$ ATCA cube centred near the NGC 2292/2293 pair; see Table 5. One of these sources is the galaxy ESO 490−G045, which was also detected in the HIPASS data. The second source found in the ATCA data is a radially narrow ring of neutral gas surrounding the pair of galaxies NGC 2292 and 2293. No H I emission was detected interior to the ring, i.e., from the region where the bulk of the optical light of the two galaxies is emitted. The optical positions and literature radial velocities of these two galaxies are given in Table 5 for reference. Two galaxies already known as members of the LGG 138 or 138* groups – NGC 2295 and ESO 490−G045 – were not detected in H I emission and are listed in Table 5 for reference.

The derived H I parameters for the seven resolved H I detections in and near LGG 138 are shown in Table 6. For the modified LGG 138 group – henceforth LGG H I 138 – which includes the seven galaxies listed in Table 6, together with the NGC 2292, 2293 and 2295 and ESO 490−G010 galaxies, which were not detected in H I emission, the following parameters pertain: the median projected galaxy–galaxy separation in the group is $400\,h_{75}^{-1}$ kpc; the median galaxy radial velocity is $2018\,\mathrm{km\,s^{-1}}$, and the median projected velocity dispersion is $213\,\mathrm{km\,s^{-1}}$. An estimate of the total dynamical group mass is $4 \times 10^{13}\,\mathrm{M_\odot}$. The median crossing time for the entire group is of order $1\,h_{75}^{-1}$ Gyr. An upper limit to the total dynamical mass-to-blue luminosity ratio of the group is $<290\,\mathrm{M_\odot/L_\odot}$. It is unlikely that the group is relaxed with all members bound.

The NGC 2292/2293 pair of galaxies was the principal target for the extended integration on LGG 138 obtained with the ATCA. Fig. 2 shows the distribution of neutral hydrogen gas relative to the optical emission of these two galaxies, and it is clear that the H I is arranged in a large-scale ring surrounding the pair. A first-order moment map shows the H I ring to be undergoing large-scale rotation with a maximum projected circular speed of $200\,\mathrm{km\,s^{-1}}$,

Table 5. H I detections (and non-detections) in the LGG 138 group for both HIPASS and ATCA data – see text for a description of the columns.

H I POSITION		LINE VELOCITY				Integrated		CATALOGUE DATA						Note(s)
RA	Dec.	V_{50}	W_{50}	V_{20}	W_{20}	flux	Galaxy	Velocity	Ref.	B_T	R_T	e	Offset	
(J2000)		($\mathrm{km\,s^{-1}}$)				($\mathrm{Jy\,km\,s^{-1}}$)		($\mathrm{km\,s^{-1}}$)					(arcmin)	
(1)	(2)	(3)	(4)	(5)	(6)	(7)	(8)	(9)	(10)	(11)	(12)	(13)	(14)	(15)
h m s	° ′ ″													
HIPASS data														
06 40 23	−27 05 33	2174	243	2159	249	19.6	ESO 490−G028	2132 ± 10	(45)	14.9	13.5	0.98	0.5	
06 44 29	−26 06 49	2461	269	2475	296	29.8	ESO 490−G037	2512 ± 3	(11)	13.0	–	0.68	1.5	
06 44 49	−27 38 28	1900	367	1895	405	202	NGC 2280	1893 ± 15	(45)	11.1	9.8	0.89	0.1	
06 46 24	−26 05 48	2355	463	2353	477	27.4	ESO 490−G041	2348 ± 20	(76)	13.5	12.0	0.95	0.9	
06 46 48	−26 27 54	1713	196	1709	225	29.4	ESO 490−G045	1694 ± 10	(45)	14.0	13.3	–	0.6	
06 46 50	−27 17 49	2208	304	2206	320	11.2	ESO 490−G044	2163 ± 13	(24)	14.3	13.3	0.84	1.7	
06 47 20	−25 37 59	2833	236	2832	249	13.4	ESO 490−G046	–	–	–	–	–	1.1	(a)
06 55 29	−26 39 05	2060	263	2056	281	28.0	ESO 491−G009	2055 ± 20	(68)	14.8	13.6	–	2.8	
ATCA data														
06 46 47	−26 28 33	1708	190	1708	214	24.9	ESO 490−G045	1694 ± 10	(45)	14.0	13.3	–	0.1	(b)
06 47 43	−26 44 54	2045	351	2043	397	8.5	–	–	–	–	–	–	–	(c)
Non-detections														
06 31 57	−26 46 09	–	–	–	–	–	ESO 490−G010	1827 ± 10	(45)	13.7	12.3	0.87	–	(d)
06 47 24	−26 44 09	–	–	–	–	–	NGC 2295	1823	(10)	13.6	11.9	0.96	–	(d, f)
06 47 40	−26 44 47	–	–	–	–	–	NGC 2292	2321 ± 37	(18)	11.8	10.4	–	–	(e, f)
06 47 43	−26 45 11	–	–	–	–	–	NGC 2293	1978 ± 32	(18)	11.7	–	–	–	(e, f)

(10) Bottinelli et al. (1992)
(11) Bottinelli et al. (1993)
(18) de Vaucouleurs et al. (1991)
(24) Garcia et al. (1994)
(45) Mathewson & Ford (1996)
(68) Takata et al. (1994)
(76) Yamada et al. (1994)

Table 6. Adopted recessional velocities and maximum deprojected circular speeds, H I masses, and H I mass to total B and R luminosity ratios for galaxies in the LGG 138 group. Limits are given where the inclination of the galaxy is not known.

Galaxy	cz ($\mathrm{km\,s^{-1}}$)	$V_{\rm circ}$ ($\mathrm{km\,s^{-1}}$)	H I mass ($10^9\,h_{75}^{-2}\,\mathrm{M_\odot}$)	$M_{\rm H\,I}/L_B$ ($\mathrm{M_\odot/L_\odot}$)	$M_{\rm H\,I}/L_R$ ($\mathrm{M_\odot/L_\odot}$)
ESO 490−G028	2159	127	4.8	1.7	1.4
ESO 490−G037	2475	218	9.5	0.65	–
NGC 2280	1895	228	38	0.67	0.60
ESO 490−G041	2353	251	8.0	0.72	0.56
ESO 490−G045	1709	>113	4.5	<1.8	<2.7
ESO 490−G044	2206	190	2.9	0.75	0.84
ESO 491−G009	2056	>140	6.3	<3.5	<3.4

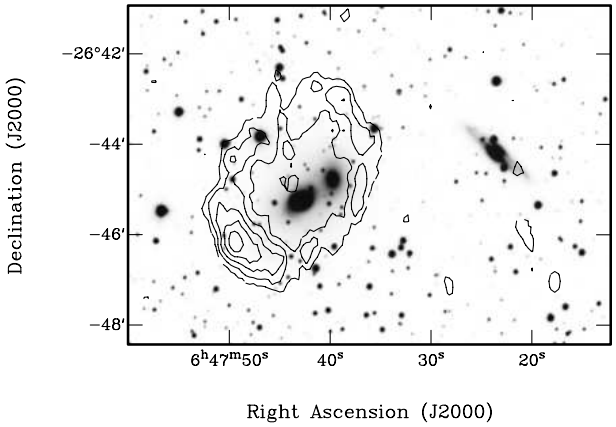

Figure 2. The H I column density distribution of the H I ring in LGG 138 (contours) overlaid on to a broad-band V image of the NGC 2292/2293 pair and NGC 2295 to the west. The contours are at levels of 1, 2, 3, 4 and $5\times10^{20}\,\mathrm{cm^{-2}}$. The overlaid H I map has been corrected for primary beam fall-off away from the pointing centre.

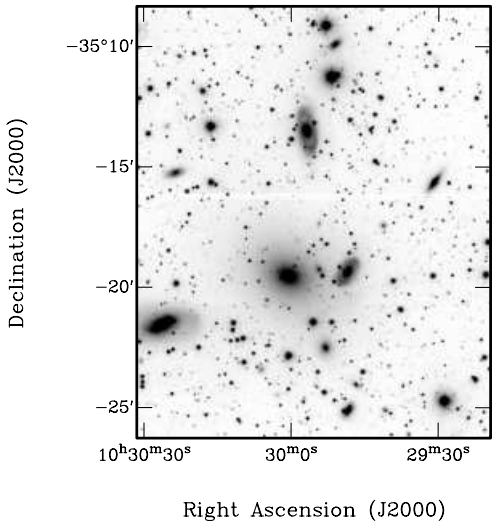

Figure 3. A broad-band V image of the three-member LGG 202 compact group.

or expansion with a projected expansion speed of $200\,\mathrm{km\,s^{-1}}$, or, as is more likely, a combination of both rotation and expansion. At an assumed distance of $27\,h_{75}^{-1}$ Mpc, the major and minor projected diameters of the ring are $\sim30\,h_{75}^{-1}$ kpc and $\sim21\,h_{75}^{-1}$ kpc respectively. The H I mass of the ring, derived from the parameters listed in Table 5, is $1.9\times10^9\,h_{75}^{-2}\,\mathrm{M_\odot}$, typical of the quantity of neutral hydrogen bound to a typical early-type spiral (Roberts & Haynes 1994). The ATCA observations reach a 3σ column density sensitivity of $1.4\times10^{19}\,\mathrm{cm^{-2}}$ *per 13.2 km s^{-1} channel*, and with no detection of H I at this level directly associated with the optical galaxies, the H I masses of the encircled galaxies NGC 2292 and 2293 are constrained to be less than $9\times10^6\,h_{75}^{-2}\,\mathrm{M_\odot}$ each for 10σ detections extending over $150\,\mathrm{km\,s^{-1}}$. There *is* low-level H I emission seen decreasing smoothly and rapidly towards the centre of the ring, but as the galaxies are not themselves centred in the ring, and the decreasing H I profile appears unaffected in the vicinity of the galaxy nuclei, the data are consistent with the ring actually being narrower than the synthesized beam, i.e., the ring thickness $\delta r \lesssim 4$ kpc or, alternatively, $\delta r/r \lesssim 0.25$, where r is the radius of the ring. For column densities above $10^{20}\,\mathrm{cm^{-2}}$, $\delta r/r \simeq 0.3$, and thus the ring is believed to be radially thin. The LGG 138 H I ring is discussed in greater detail in Barnes (1999).

5.2 LGG 202

No H I emission was detected in the ATCA data set for this group. Whilst the integration time acquired with the telescope was less for LGG 202 than for the four other groups, the group is at only an intermediate redshift, and spiral galaxies at this distance having normal H I contents would be detected in these observations. For example, a galaxy having a velocity width of $\sim200\,\mathrm{km\,s^{-1}}$ and an H I mass of $10^8\,h_{75}^{-2}\,\mathrm{M_\odot}$ would be at the limit of detectability at the phase centre of the observations. Away from the pointing centre, or for resolved galaxies, a greater mass or narrower velocity width would be required for detection. That is to say, more realistic upper estimates of the gas mass which could be in each of the three LGG 202 galaxies, yet not detected in the ATCA images, are gas masses of order $10^9\,h_{75}^{-2}\,\mathrm{M_\odot}$. The broad-band V image of the LGG 202 group acquired with the MSO 40-inch telescope is shown in Fig. 3.

This group is deficient in neutral hydrogen. The compact group LGG 202 as classified by Garcia (1995) comprises the three galaxies NGC 3267, 3269 and 3271. The galaxies are classified as early-type spirals, and the latter two are barred (de Vaucouleurs et al. 1991). NGC 3269, at (J2000) RA $10^{\rm h}29^{\rm m}58^{\rm s}$, Dec. $-35°13'24''$ in Fig. 3, has been previously recognized as having a ring (Corwin et al. 1985), whilst NGC 3271, at (J2000) RA $10^{\rm h}30^{\rm m}27^{\rm s}$, Dec. $-35°21'31''$, has been studied by Bettoni & Galletta (1997), who remark that the bar extends for a significant fraction of the disc scalelength, and is delineated by dust lanes at either end of the bar where the beginnings of two spiral arms can be seen. The total blue (Cousins) magnitudes of the three galaxies (in the order listed above) are 13.5, 13.2 and 12.7, yielding upper limits to the H I mass-to-blue light ratios for the LGG 202 galaxies – NGC 3267, 3269 and 3271 – of order 3×10^{-2} solar units each. These H I

Table 7. H I detections in the CCG 1 group for both HIPASS and ATCA data – see text for a description of the columns.

H I POSITION		LINE VELOCITY				Integrated		CATALOGUE DATA						Note(s)
RA	Dec.	V_{50}	W_{50}	V_{20}	W_{20}	flux	Galaxy	Velocity	Ref.	B_T	R_T	e	Offset	
(J2000)		($km\,s^{-1}$)				($Jy\,km\,s^{-1}$)		($km\,s^{-1}$)					(arcmin)	
(1)	(2)	(3)	(4)	(5)	(6)	(7)	(8)	(9)	(10)	(11)	(12)	(13)	(14)	(15)
h m s	° ′ ″													
HIPASS data														
12 40 52	−36 44 53	3285	200	–	–	28.9	AM 1238−362	–	–	–	–	–	0.4	(a)
12 43 54	−36 31 41	3311	199	3304	229	14.0	ESO 381−G014	3305 ± 10	(45)	15.2	14.0	0.98	3.3	
ATCA data														
12 40 41	−36 44 22	3102	153	3101	177	3.2	ESO 381−G006	–	–	15.9	14.9	0.99	0.1	
12 40 53	−36 45 27	3284	171	3282	219	7.0	ESO 381−G008	3285 ± 7	(1)	13.0	11.9	0.30	0.1	
12 40 58	−36 43 52	3287	168	3288	190	7.7	ESO 381−G009	3050 ± 190	(18)	13.9	12.7	0.66	0.1	

(1) Agüero et al. (1994)
(18) de Vaucouleurs et al. (1991)
(45) Mathewson & Ford (1996)

Table 8. Adopted recessional velocities and maximum deprojected circular speeds, H I masses, and H I mass to total B and R luminosity ratios for galaxies in the CCG 1 group. Limits are given where the inclination of the galaxy is not known.

Galaxy	cz ($km\,s^{-1}$)	V_{circ} ($km\,s^{-1}$)	H I mass ($10^9\,h_{75}^{-2}\,M_\odot$)	M_{HI}/L_B ($M_\odot/L_\odot$)	M_{HI}/L_R ($M_\odot/L_\odot$)
ESO 381−G006	3101	89	1.5	0.64	0.75
ESO 381−G008	3282	>110	3.6	<0.17	<0.18
ESO 381−G009	3288	144	4.0	0.39	0.39
ESO 381−G014	3304	117	7.3	1.6	1.6

mass-to-light ratios may be low for two reasons. The H I in the group may be dispersed over a region several hundred kpc across, and extending several hundred $km\,s^{-1}$ in velocity space. This would render the synthesis observations blind to H I, and could in principle exist at a low enough column density to prevent detection even in the HIPASS data. Conversely, H I may simply be absent from the group, having either been depleted by rapid star formation at an early epoch, or dispersed into a hot intracluster medium enhanced by many close encounters in the dense group environment. The latter seems likely, given that the LGG 202 group is embedded in a dense condensation of galaxies within the Antlia cluster. Supporting this hypothesis, publicly available *ROSAT* X-ray images of the LGG 202 region obtained with the PSPC instrument indicate a diffuse X-ray-emitting medium spread in a halo centred nearly exactly on the optical group centre.

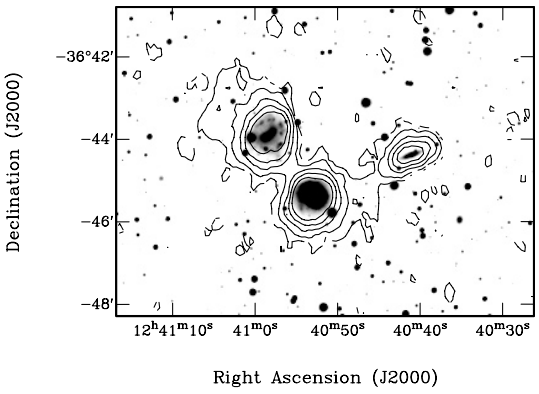

Figure 4. The H I column density distribution of the neutral hydrogen in CCG 1 (contours) overlaid on a broad-band V image of the three-member group. The contours are at levels of 1.0, 2.5, 5.0, 7.5 and $10 \times 10^{20}\,cm^{-2}$. The overlaid H I map has been corrected for primary beam fall-off away from the pointing centre.

5.3 CCG 1

Two H I sources were found in the $4° \times 4° \times 2700\,km\,s^{-1}$ HIPASS cube centred on the AM 1238-362 triplet in CCG 1. The measured parameters of these galaxies are shown in Table 7; the columns are the same as those in Table 5, with the exception of the notes, which follow.

Column (15). Notes:

(a). AM 1238-362 is the dense triplet that CCG 1 includes, and was unresolved in the HIPASS data. The central velocity and width of the triplet have been read by eye from an integrated HIPASS spectrum of the region encompassing the three sources, and consequently are only approximate.

The three members of the AM 1238-362 triplet were resolved in neutral hydrogen emission by the ATCA observations; see Table 7. ESO 381−G014, which was detected in the CCG 1 HIPASS cube at a velocity consistent with it being a new member of the CCG 1 group, was not within the ATCA field of view, and consequently was not imaged at high resolution. The derived H I parameters for the total of four galaxy detections near CCG 1 are shown in Table 8. These four galaxies are adopted as the members of the CCG H I 1 group, having a median radial velocity of $3285\,km\,s^{-1}$; a median projected velocity dispersion of $11\,km\,s^{-1}$; and a median projected galaxy–galaxy displacement of $110\,h_{75}^{-1}\,kpc$. The median crossing time is of order $10\,h_{75}^{-1}\,Gyr$. The total dynamical mass of the group is estimated to be $\sim 10^{12}\,M_\odot$, and the total dynamical mass-to-blue luminosity ratio is constrained to be $<30\,M_\odot/L_\odot$.

The triplet AM 1238-362 was the principal target for the ATCA observations of CCG 1. Fig. 4 shows the neutral hydrogen column density overlaid on the optical emission of the galaxies, and the 21-cm spectral line emission is seen to be confined to the three

Table 9. H I detections and non-detections in the HCG 91 group for both HIPASS and ATCA data – see text for a description of the columns.

H I POSITION		LINE VELOCITY				Integrated		CATALOGUE DATA						Note(s)
RA	Dec.	V_{50}	W_{50}	V_{20}	W_{20}	flux	Galaxy	Velocity	Ref.	B_T	R_T	e	Offset	
(J2000)		($km\,s^{-1}$)				($Jy\,km\,s^{-1}$)		($km\,s^{-1}$)					(arcmin)	
(1)	(2)	(3)	(4)	(5)	(6)	(7)	(8)	(9)	(10)	(11)	(12)	(13)	(14)	(15)
HIPASS data														
22 04 02	−27 57 50	6157	170	6152	189	9.0	ESO 466−G049	6093 ± 10	(45)	15.5	14.8	0.56	4.8	
Non-detections or unresolved sources														
22 09 08	−27 48 35	–	–	–	–	–	NGC 7214	6934 ± 10	(37)	13.3	11.4	–	–	(a)
22 09 09	−27 48 03	–	–	–	–	–	ESO-LV 4670121	7315 ± 22	(38)	12.6	11.6	–	–	(a)
22 09 14	−27 46 55	–	–	–	–	–	ESO 467−G013	7319 ± 49	(30)	14.8	14.0	–	–	(a)
22 09 16	−27 43 50	–	–	–	–	–	ESO 467−G015	7196 ± 66	(30)	15.0	13.9	0.98	–	(a)

(31) Hickson et al. (1992)
(37) Keel (1996a)
(38) Keel (1996b)
(45) Mathewson & Ford (1996)

galaxies. Note that data used for this overlay are the uniformly weighted data, which provide sufficient resolution to resolve the gas in the three galaxies, and establish that there is very little emission seen outside the optical discs. The north-east extension of neutral gas outside the optical disc of ESO 381- G009 is real, and lies at the velocity of the peak in the 21 cm spectrum corresponding to the receding side of the galaxy. Inspection of the zeroth- and first-order moment maps shows all three galaxies to be rotating regularly. The integrated H I flux detected in the *naturally* weighted ATCA data is only 20 per cent less than that detected by Parkes, confirming that the H I is predominantly located in the discs of the galaxies, rather than concealed from the ATCA interferometer in a large smooth cloud of H I.

CCG 1 was one of the densest groups observed, yet presently appears to be free of strong galaxy interactions or mergers, consistent with the long median crossing time. The original group was determined to comprise only the three galaxies ESO 381- G006, G008 and G009, but the discovery of the galaxy ESO 381- G014 in the HIPASS cube at an identical redshift to the AM 1238-362 triplet, and at a projected distance of $\sim 0.5\,h_{75}^{-1}$ Mpc from the triplet, suggests that this is a four galaxy system. The lack of a common envelope of neutral gas surrounding the triplet, and the absence of any significant tidal tails or gas bridges, strongly suggests that the group is in fact much looser than the projected density implies – perhaps the typical true galaxy separations are more like 0.5 Mpc rather than 50 kpc. In this case, the high projected density on the sky can be explained as a chance projection of galaxies which do not form a compact group, but rather are members of a looser group. Note that CCG 1 does in fact comprise galaxies whose radial velocities place them within the Centaurus ($3000\,km\,s^{-1}$) cluster; this is proposed to be playing the part of the loose group from which the galaxies are projected densely on to the sky.

There are two indirect pieces of evidence for possible galaxy interactions in the CCG 1 group. First, ESO 381−G009, the north-eastern galaxy in the triplet (see Fig. 4), exhibits a peculiar, low column density extension of H I towards the north-east. The cause of this H I plume is unknown, but the galaxy appears to be experiencing star formation in a ring surrounding the nucleus, in a manner reminiscent of the Cartwheel ring galaxy (Higdon 1996, and references therein), and perhaps the gas has been blown out by galactic winds caused by massive star formation. Alternatively, the H I may have been dragged out of the disc in a brief high-speed encounter with another galaxy. Secondly, ESO 381−G008, the southern central galaxy in the triplet, is known to be a warm

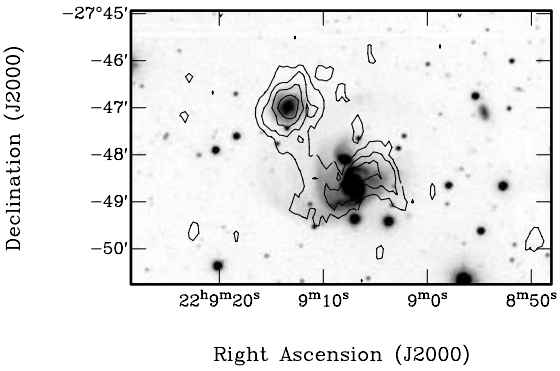

Figure 5. The H I column density distribution of the neutral hydrogen in HCG 91 (contours) overlaid on a broad-band V image of the three-member group. The contours are at levels of 1.5, 3.0, 4.5 and 6.0×10^{20} cm^{-2}. The overlaid H I map has been corrected for primary beam fall-off away from the pointing centre.

infrared emission source (de Grijp, Miley & Lub 1987). Agüero et al. (1994) measure the Hα and infrared luminosities of ESO 381−G008 to be $\log(L_{H\alpha}/L_\odot) = 7.65$ and a very high $\log(L_{IR}/L_\odot) = 10.35$ respectively, leading them to classify its nucleus as a Seyfert 2. Since there is now substantial evidence to suggest that galaxies in dense environments are more likely to experience starburst activity (Rubin, Ford & Hunter 1990; Zepf 1993; Ribeiro et al. 1996; Sanders & Mirabel 1996), the visual star formation in ESO 381−G009 and the active nucleus in ESO 381-G008 are probably evidence that the CCG 1 group, even if it is looser than projected on the sky, has a sufficiently short crossing time to at least enhance star formation via galaxy harassment (e.g. Moore et al. 1996).

5.4 HCG 91

The relatively high redshift of this group ($cz \simeq 7100\,km\,s^{-1}$) makes detection of all but the most H I massive objects difficult in the HIPASS data. Whilst there is extremely faint and diffuse emission visible at the position of HCG 91 in the HIPASS cube centred on the group, it is not sufficiently bright to extract a moment map or integrated spectrum, nor is it visible in an XPEAK map derived from the cube. The galaxy ESO 466−G049, which is not a member of the compact group, was detected to the west of HCG 91 in the HIPASS cube; see Table 9. The columns in this table are the same as those for Table 5, with the exception of the notes, which follow. This galaxy is rotating with a circular speed

of order 170 km s^{-1}, and at a radial velocity of 6152 km s^{-1} it has an H I mass of $1.4 \times 10^{10}\, h_{75}^{-2}\, M_{\odot}$. The ratio of H I mass to blue luminosity for ESO 466−G049 is calculated to be $1.8\, M_{\odot}/L_{\odot}$, making it moderately H I-rich.

Column (15). Notes:

(a). The positions given for these galaxies are previously measured optical positions.

The ATCA data for HCG 91 shows H I emission centred on the two galaxies ESO 467−G013 and NGC 7214, which are optically the brightest members of the group – see Fig. 5. Whilst the detection is of moderate signal-to-noise ratio in the naturally weighted data, it is not of significant resolution to resolve the H I into discrete discs. Conversely, the uniformly weighted data gives too high a noise level to allow confident integration of fluxes. Whilst the column density and velocity field maps suggest that the ESO 467−G013 and NGC 7214 are resolved, the maps have been

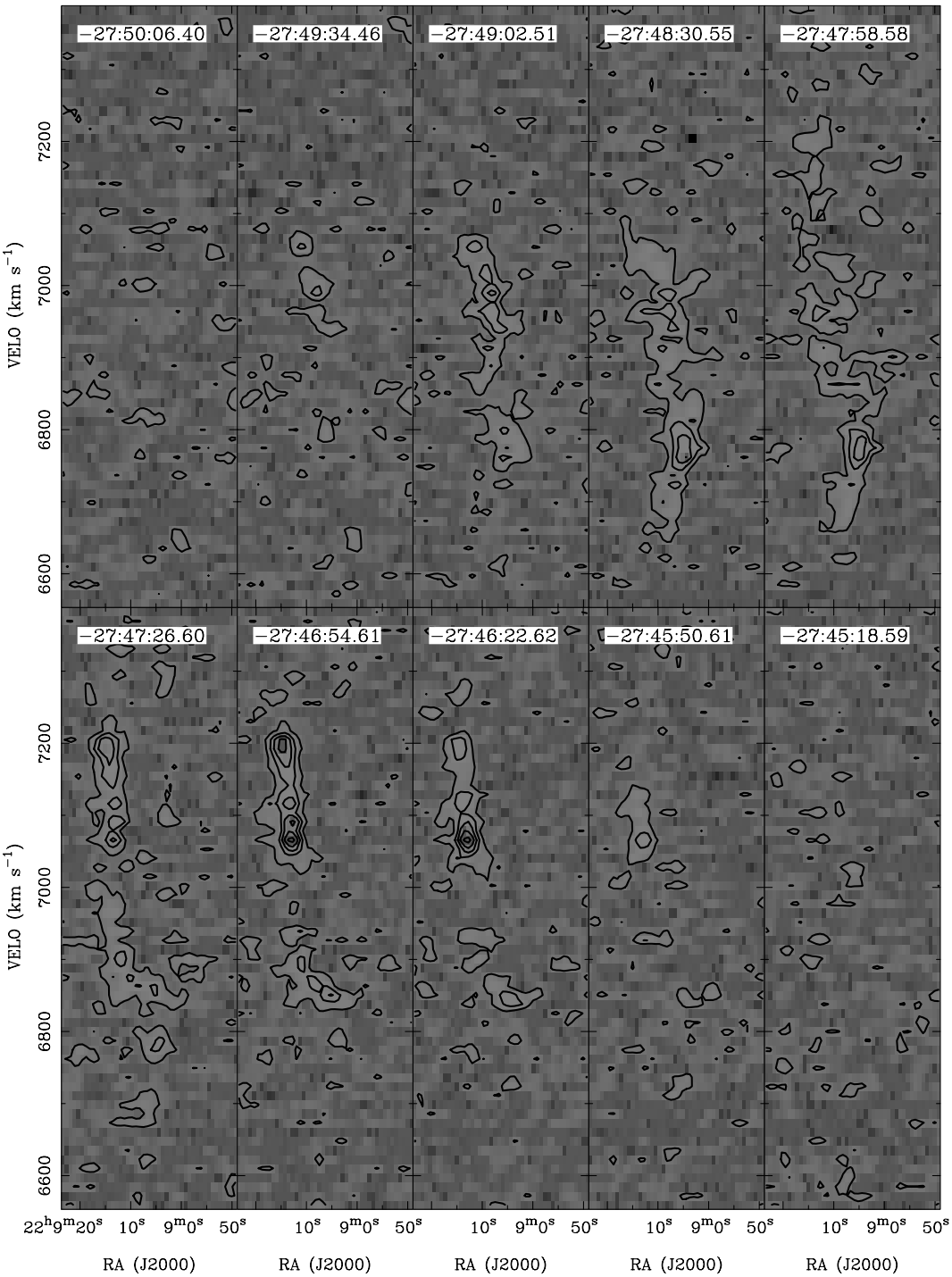

Figure 6. H I position–velocity maps of NGC 7214, ESO 467−G013 and ESO-LV 4670121 in HCG 91. Each map is the average of two adjacent RA–velocity planes in the position–velocity cube. The contour levels are at 2, 5, 7.5, 10 and 12.5 mJy beam^{-1}; the velocity scale is in radio convention – for optical velocities add ∼170 km s^{-1}. The average Dec. of each plane is indicated at the top of each panel.

generated from masked data sets, and inspection of the *unmasked* data sets show the emission to be diffuse. Fig. 6 shows a number of slices along the declination direction for ESO 467−G013 and NGC 7214; which H I 'belongs' to which galaxy cannot be confidently established. Consequently, extraction of individual galaxy parameters is not possible for this system. However, the *total* H I flux from the group can be determined using the histogram subtraction method (Barnes 1998), which yields a flux of $8.8\,\mathrm{Jy\,km\,s^{-1}}$, corresponding to a total H I mass of the group of $1.9\times10^{10}\,h_{75}^{-2}\,\mathrm{M}_\odot$. The members of the HCG 91 group which were not detected or resolved in H I emission (i.e., *all* previously known members of HCG 91) are listed in Table 9 for reference.

Optically, the galaxies NGC 7214 and ESO-LV 4670121 are nearly superimposed, and tidal tails resembling loosely wound spiral arms are visible, reaching beyond 3 times the optical radius of NGC 7214, which is the bright galaxy in the south of Fig. 5. These galaxies are extremely likely to be interacting, with Hα emission visible in the east of NGC 7214, and warm infrared detections of the system. The northern tidal arm passes to the south of the galaxy ESO 467−G013 at a projected distance of only 30 arcsec, or $\sim14\,h_{75}^{-1}$ kpc, from the centre of the galaxy, suggesting that ESO 467−G013 may also be participating in the interaction.

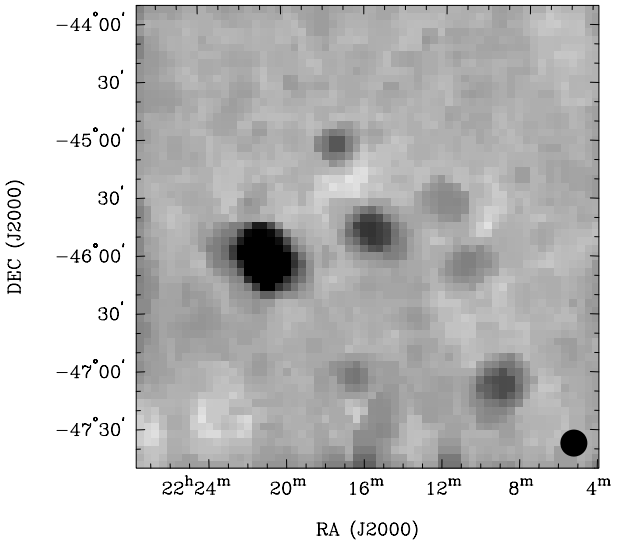

Figure 7. Peak H I intensity map of LGG 455 derived from spatially smoothed HIPASS data. The 14.4-arcmin observing beam is shown in the lower right corner.

There is weak evidence for the detection of this tidal arm in H I emission. In Fig. 6, NGC 7214 appears as the single bright emission spot in the fourth and fifth panels (i.e., those labelled −27 48 30.55 and −27 47 58.58) near $6750\,\mathrm{km\,s^{-1}}$. ESO 467−G013 is the double horned object in panels 6 to 8 at 7070–7200 $\mathrm{km\,s^{-1}}$. The remaining H I distribution appears to be a string of clouds at (J2000) RA $22^{\mathrm{h}}09^{\mathrm{m}}10^{\mathrm{s}}$ spread out in velocity space from 6650–7250 $\mathrm{km\,s^{-1}}$. The position of these detections would be marginally consistent with their assocation with the northern optical tidal arm. The broken nature of this collection of gas clouds is likely due to low signal-to-noise ratio for these detections, and further imaging may show a connected stream of H I.

Despite the merging and interaction occurring in HCG 91, the group is still relatively rich in neutral gas. This is more surprising in the light of the detection of soft X-ray emission from the group (Ebeling et al. 1994), which would be expected to heat and ionize the neutral hydrogen in the group. However, if the hot gas responsible for the X-ray emission is confined to the Seyfert 1 nucleus of the first-ranked galaxy, NGC 7214, then the neutral gas in the disc of NGC 7214 and in the remainder of the group will remain unaffected. This possibility is strongly supported by Ebeling et al., who note that the *ROSAT*-detected X-ray emission from HCG 91 is point-like. The ATCA observations detect a total H I mass of $2\times10^{10}\,h_{75}^{-2}\,\mathrm{M}_\odot$ in the vicinity of the three galaxies NGC 7214, ESO 467−G013 and ESO-LV 4670121. The total H I mass-to-blue luminosity ratio for the group is $\lesssim0.1\,\mathrm{M}_\odot/\mathrm{L}_\odot$. Since

Table 10. H I detections (and non-detections) in the LGG 455 group for both HIPASS and ATCA data – see text for a description of the columns.

H I POSITION		LINE VELOCITY				Integrated		CATALOGUE DATA						Note(s)
RA	Dec.	V_{50}	W_{50}	V_{20}	W_{20}	flux	Galaxy	Velocity	Ref.	B_T	R_T	e	Offset	
(J2000)		($\mathrm{km\,s^{-1}}$)				($\mathrm{Jy\,km\,s^{-1}}$)		($\mathrm{km\,s^{-1}}$)					(arcmin)	
(1)	(2)	(3)	(4)	(5)	(6)	(7)	(8)	(9)	(10)	(11)	(12)	(13)	(14)	(15)
HIPASS data														
22 09 10	−47 09 21	1748	161	1755	359	43.7	NGC 7213	1803 ± 32	(18)	11.0	–	0.35	1.2	
22 10 49	−46 05 00	2840	335	2831	360	27.7	ESO 288−G046	2847 ± 5	(12)	13.5	12.2	–	1.3	
22 12 03	−45 33 42	1969	139	1960	196	10.5	ESO 288−G049	1969 ± 10	(45)	14.0	13.3	–	3.0	
22 15 34	−45 49 26	1930	660	–	–	51.7	AM 2212-460	–	–	–	–	–	1.8	(a)
22 16 40	−47 05 24	2765	213	2768	235	13.8	ESO 289−G010	2783 ± 10	(45)	14.8	13.9	0.99	1.8	
22 17 13	−45 03 46	1820	112	1822	126	13.0	ESO 289−G011	1822 ± 20	(15)	14.9	13.9	–	0.6	
22 20 56	−46 02 24	915	190	915	209	216	ESO 289−G018	918 ± 10	(45)	11.5	10.7	0.91	0.4	
ATCA data														
22 15 35	−45 51 02	1735	231	1727	263	3.5	NGC 7232	1796 ± 30	(18)	12.6	11.0	–	0.5	
22 15 53	−45 46 50	2160	62	2162	81	7.2	NGC 7232B	2042 ± 8	(42)	13.5	12.6	–	0.1	
Non-detections or unresolved sources														
22 13 22	−46 01 00	–	–	–	–	–	ESO 289−G001	1987 ± 24	(15)	12.4	10.9	0.94	–	(b)
22 15 49	−45 50 50	–	–	–	–	–	NGC 7233	1841 ± 7	(66)	12.9	11.8	0.43	–	(b)

(12) Chengalur, Salpeter & Terzian (1993)
(15) da Costa et al. (1991)
(18) de Vaucouleurs et al. (1991)
(42) Lauberts & Valentijn (1989)
(45) Mathewson & Ford (1996)
(66) Strauss et al. (1992)

Table 11. Adopted recessional velocities and maximum deprojected circular speeds, H I masses, and H I mass to total B and R luminosity ratios for galaxies in the LGG 455 group. Limits are given where the inclination of the galaxy is not known.

Galaxy	cz ($\mathrm{km\,s^{-1}}$)	$V_{\rm circ}$ ($\mathrm{km\,s^{-1}}$)	H I mass ($10^9\,h_{75}^{-2}\,\mathrm{M_\odot}$)	$M_{\rm H\,I}/L_B$ ($\mathrm{M_\odot/L_\odot}$)	$M_{\rm H\,I}/L_R$ ($\mathrm{M_\odot/L_\odot}$)
NGC 7213	1755	>180	5.8	<0.16	–
ESO 288−G046	2831	>180	9.6	<1.1	<0.93
ESO 288−G049	1960	>98	1.8	<0.63	<0.98
NGC 7232	1727	>132	0.45	<0.06	<0.04
NGC 7232B	2162	>40	1.4	<0.27	<0.35
ESO 289−G010	2768	119	4.5	1.0	1.3
ESO 289−G011	1822	>63	1.9	<1.8	<2.1
ESO 289−G018	915	115	7.8	1.0	1.4

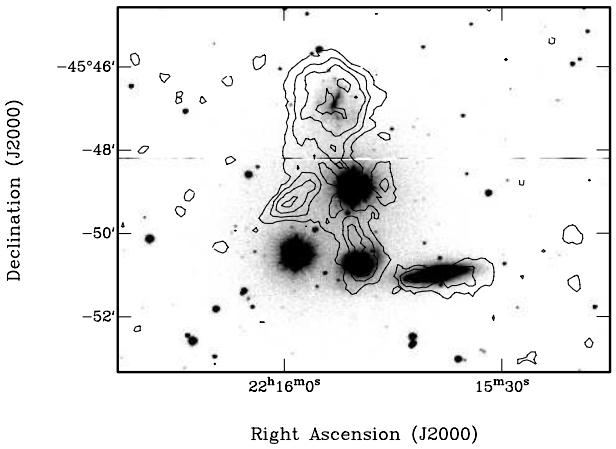

Figure 8. The H I column density distribution of the neutral hydrogen in LGG 455 (contours) overlaid on a broad-band V image of the three-member group. The contours are at levels of 2, 4, 6 and $8\times10^{20}\,\mathrm{cm^{-2}}$. The overlaid H I map has been corrected for primary beam fall-off away from the pointing centre. Note that the there are two bright stars in this image, one located near RA $22^{\rm h}15^{\rm m}55^{\rm s}$, and the other near Dec. $-45°49'00''$.

the group is angularly small, there is unlikely to be any significant flux on spatial scales to which the ATCA interferometer was insensitive, so the H I mass reported is probably within 20 per cent of the actual value, neglecting the possibility of self-absorption by the neutral gas.

5.5 LGG 455

Seven sources were detected in H I emission in the $4°\times4°\times2670\,\mathrm{km\,s^{-1}}$ HIPASS cube centred on the AM 2212-460 triplet in LGG 455 – see Fig. 7. The measured parameters of these sources are shown in Table 10; the columns are the same as those in Table 5, with the exception of the notes, which follow.

Column (15). Notes:

(a). AM 2212-460 is the dense triplet that LGG 455 includes, and was unresolved in the HIPASS data. The central velocity and width *of the triplet* have been read by eye from an integrated HIPASS spectrum of the region encompassing the three sources, and consequently are only approximate.

(b). The positions listed are previously known optical positions.

Disturbed H I was detected in the $40\times40\,\mathrm{arcmin^2}\times1000\,\mathrm{km\,s^{-1}}$ ATCA cube centred on the triplet AM 2212-460; see Table 10. As well as H I emission directly associated with each of the members of the triplet, there is a plume of H I spanning an arc between two of the galaxies (see below). Of the four galaxies previously assigned as members of the LGG 455 group, three – NGC 7232, 7232B and 7233 – were detected in H I. ESO 289-G001 was not detected, although it is within the position–velocity space imaged by both instruments; previous observations have set an upper limit to the H I flux from this object of $5.2\,\mathrm{Jy\,km\,s^{-1}}$ (Huchtmeier & Richter 1989). Integrated H I data are not listed for NGC 7233, since the neutral gas distribution in its vicinity is too disturbed to confidently differentiate between galactic and extragalactic 'blobs' of H I emission in the channel maps. Besides those galaxies already assigned to the LGG 455 group, the HIPASS observations detect a further six galaxies in the vicinity of the group, at recessional velocities displaced by up to $1000\,\mathrm{km\,s^{-1}}$ from the centre of the compact core of the group. The derived H I parameters of the total of eight galaxies detected individually in H I are shown in Table 11. Excluding the galaxies ESO 288- G046 and ESO 289- G010 and G018, the remaining galaxies listed in Table 11, together with NGC 7233 and ESO 289- G001 (which was not detected), are accepted as members of the group LGG H I 455. This group has a median radial velocity of $1841\,\mathrm{km\,s^{-1}}$ and a velocity dispersion of $114\,\mathrm{km\,s^{-1}}$. The median projected galaxy–galaxy displacement is $\sim320\,h_{75}^{-1}$ kpc, and the group dynamical mass is estimated to be $10^{13}\,\mathrm{M_\odot}$. The total mass-to-light ratio, as determined from the dynamical mass, and inclination-corrected magnitudes, is $\sim100\,\mathrm{M_\odot/L_\odot}$. For the entire group, the median crossing time is of order 2.5 Gyr.

The triplet AM 2212-460 was the principal target for the ATCA observations of LGG 455. Fig. 8 shows the distribution of neutral hydrogen gas relative to the optical emission of the galaxies, and emission is seen both in the individual galaxies, as well as in an extended plume connecting the two eastern-most galaxies, and possibly faintly reaching the western galaxy. The velocity field of the H I in the triplet indicates regular rotation in the south-west galaxy NGC 7232, disturbed rotation in the north-eastern galaxy NGC 7232B, and an irregular velocity structure in NGC 7233. The plume does not appear to be rotating, and lies midway between the radial velocities of the two eastern galaxies. H I emission extends patchily through the velocity planes from the position and velocity of NGC 7233 ($\sim1785\,\mathrm{km\,s^{-1}}$) north-east to the main eastern cloud at $\sim1880\,\mathrm{km\,s^{-1}}$. There are small patches of H I emission stretching north-west of the cloud heading back towards NGC 7232B, but these detections are probably only at the 2σ to 3σ level. Since the H I structure in this group is complex, individual channels maps are given in Fig. 9 to show the distribution of neutral gas at various velocities.

The dense triplet in LGG 455 appears to be embedded in a group comprising at least four other galaxies, as shown by the

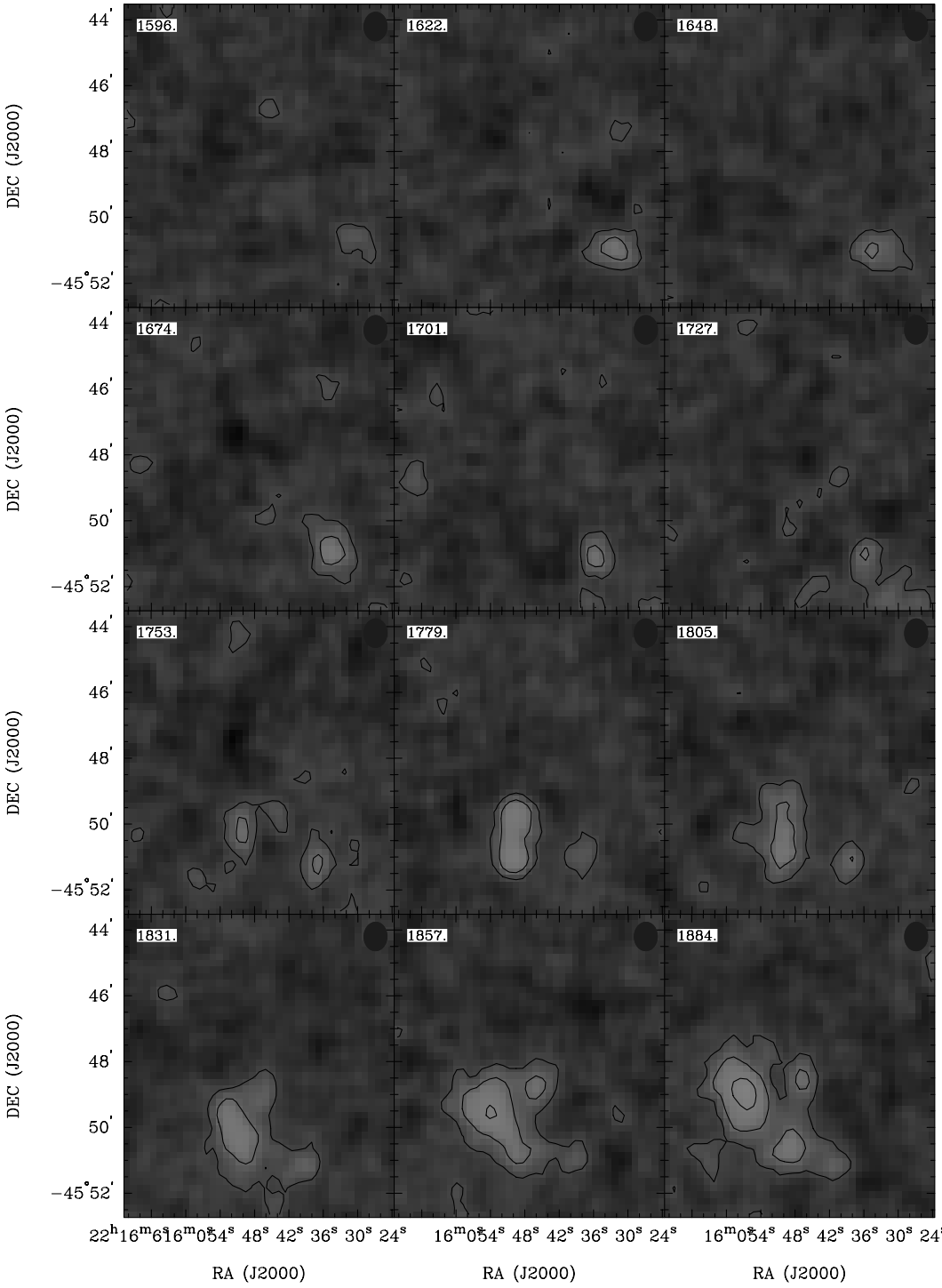

Figure 9. Clean H I channel maps of the AM 2212-460 triplet in LGG 455. The channels have been averaged two at a time to enhance the signal-to-noise ratio for presentation purposes. The contour levels are at 2, 5, 10 and 20 mJy beam^{-1}; the barycentric radio velocity of each plane is shown in the upper right corner of each map (the optical velocities are $\sim$11 km s^{-1} higher than those shown). The map has not been corrected for primary beam fall-off, since it is very near the pointing centre for the observations.

HIPASS observations. The median projected galaxy displacement of $320\,h_{75}^{-1}$ kpc for all seven galaxies is lowered by an order of magnitude to $30\,h_{75}^{-1}$ kpc when only the triplet galaxies – NGC 7232, 7232B and 7233 – are considered, leading to a reduced crossing time of order $230\,h_{75}^{-1}$ Myr for the triplet. The H I in this group is clearly disturbed, with a substantial fraction of the gas residing exterior to the galaxies, including a large concentration of gas resident in the plume described above. Furthermore, there is a severe deficit of 21-cm flux in the ATCA data (18 Jy km s^{-1}) compared to the HIPASS data (52 Jy km s^{-1}; Table 10), and this 'missing' flux is most easily explained by the synthesis data being insensitive to low-frequency components of the emission distribution across the sky. The total H I mass detected by the Parkes telescope is $8.2 \times 10^9\,h_{75}^{-2}\,M_\odot$, and it is feasible that this mass

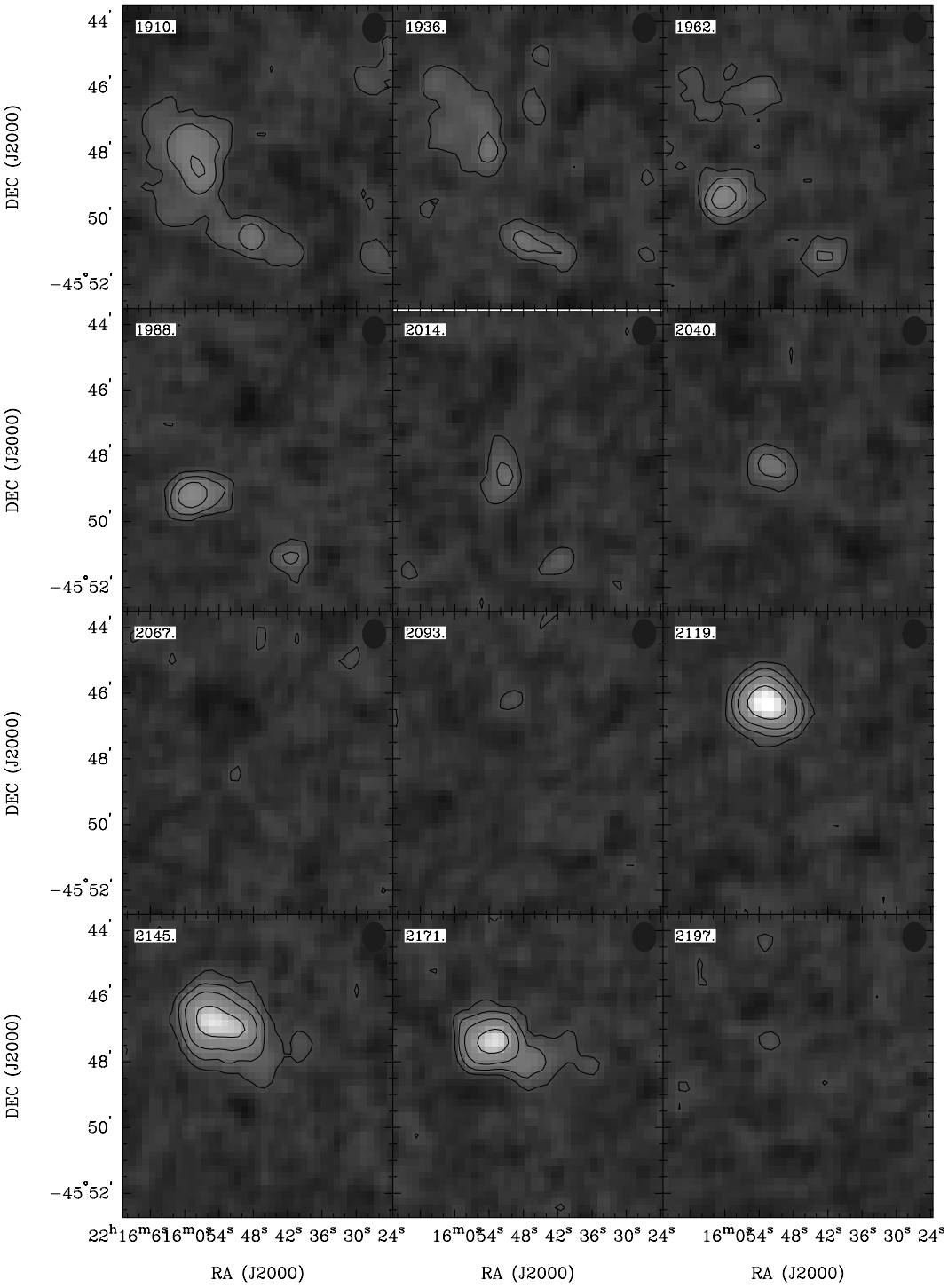

Figure 9 – *continued*

represents the gas mass of three galaxies, a large fraction of which has been tidally or ram-pressure stripped from the galactic discs and distributed smoothly throughout a common 'halo' enveloping the three galaxies. Given the disturbed H I structure, the evidence for a diffuse halo of H I, and the very dense nature of the triplet on the sky and its moderate velocity spread, it is surmised that the AM 2212-460 triplet, unlike AM 1238-362 in CCG 1, is physically dense, and not merely a manifestation of projection effects. It clearly resides within a larger, looser agglomeration of galaxies.

The peak column density detected by the ATCA in the eastern gas cloud, or plume, which is centred at (J2000) RA $22^{h}15^{m}59^{s}$, Dec. $-45°49'08''$, is $8.5 \times 10^{20}\,\mathrm{cm}^{-2}$ or, in alternative units, $6.8\,\mathrm{M}_{\odot}\,\mathrm{pc}^{-2}$. This is well in excess of the critical surface density for star formation (Kennicutt 1989), yet there is no catalogued galaxy at this position. Unfortunately, the presence of two bright stars superimposed on the triplet makes identification of any stellar population associated with this cloud extremely difficult. In principle, the stars could be subtracted from an optical image,

provided that a good model for the point spread function of the imaging instrument is known. However, this is not possible with the MSO 40-inch data. The total mass of gas within the cloud is $\gtrsim 4 \times 10^8 \, h_{75}^{-2} \, M_\odot$.

6 DISCUSSION

The compact groups in existing catalogues are made up of physically dense systems, together with chance projections of galaxies selected from looser systems. While this is somewhat obvious, it is important to note that in this study, two specific systems which are close to being optically indistinguishable *and* which show velocity concordance, have been identified as likely being quite different physically. The AM 2212-460 triplet in LGG H I 455 is a clear example of a triplet that is truly physically dense and embedded in a looser system comprising several galaxies. This group typifies the findings of Rood & Struble (1994) (amongst others) that a large number of the observed Hickson compact groups are found in looser systems. The compact core of the group has surely evolved substantially from its original state, yet the remainder of the galaxies in the group may not yet be relaxed in the group potential, and certainly show no signs of abnormality in H I content or optical morphology. The galaxies in the group presumably formed normally in sharp and deep potentials, but those in the dense core of galaxies are beginning to coalesce to form a single, smooth potential throughout which a substantial fraction of the neutral gas content of the three galaxies is already dispersed. Over the next few Gyr the three galaxies in AM 2212-460 can be expected to merge to form a single elliptical or cD type galaxy.

Conversely, the probability of chance projections within a narrow solid angle of galaxies having accordant radial velocities is greatly increased for sight lines passing through loose, rich groups and clusters, over that for random sight lines through the general field of galaxies. The AM 1238-362 triplet in CCG H I 1 is probably a good example of this effect. The three galaxies taken together easily satisfy the Hickson (1982) and Hickson et al. (1992) criteria as an apparent compact group, yet exhibit little evidence for strong past or present galaxy–galaxy interactions. Since the positions and radial velocities of the three galaxies in the triplet place them in the $3000 \, km \, s^{-1}$ Centaurus cluster, it is natural to conclude that the group is a projection of three galaxies that are physically unrelated.

Technically, the H I contents of these two triplets as measured by the synthesis observations compared to the single-dish observations suggest a new diagnostic for the physical state of a group. The synthesis flux measured for the AM 1238-362 galaxy triplet in CCG 1 is depressed by only about 20 per cent from the flux recorded in the HIPASS data, whilst the synthesis flux for the AM 2212-460 triplet in LGG 455 is lower than the HIPASS flux by 65 per cent. The maximum angular extents of H I in AM 1238-362 and AM 2212-460 are $\sim$5 and $\sim$6 arcmin respectively, i.e., the groups are nearly identical in angular scale, and indeed complexity, since they each contain three or four principal clouds of H I. Consequently, given the much greater 'missing' flux in the LGG 455 triplet compared to that in the CCG 1 triplet, it must be concluded that the H I distribution in AM 2212-460 is significantly smoother, i.e., contains a high fraction of flux at low spatial frequencies, than the gas distribution in AM 1238-362. It may also be true that H I extends smoothly well beyond the $\sim$6-arcmin H I extent of AM 2212-460 visible in the synthesis data; either way, there is clearly an excess of H I distributed diffusely throughout the dense triplet, *outside* of the galaxy discs. Thus the comparison of single-dish H I integrated fluxes to those determined from synthesis observations is proposed as a new measure of assessing whether a system is embedded in a common halo of H I. Of course, in practice, it may often be impossible to tune the array spacings to compare systems subtending different areas on the sky.

Large H I shell structures, like those seen by Malin & Hadley (1997) can potentially form within compact groups. The large-scale, radially thin ring detected in LGG 138 may be a cross-section through a presently forming shell structure. In this scenario, after a few Gyr the two enclosed galaxies will have merged, leaving an irregular or elliptical remnant at the centre of a shell of H I gas. The shell would probably contain young stars – stars that are presently forming in the south-eastern part of the ring (see Barnes 1999). Further work, especially numerical modelling, will contribute significantly to our understanding of H I shell structures.

With respect to the proposed H I deficiency of group galaxies, this study can only contribute further examples of groups which are deficient in H I content (e.g., LGG 202), and groups which are essentially normal (e.g., CCG 1). Further work on an H I-selected sample of galaxies will be necessary to establish whether H I deficiency in galaxy groups is a real effect, and what the causes of such deficiency might be.

Putting H I deficiency to one side, weak but long-term tidal effects can surely at least displace or distort neutral gas discs relative to the stellar population in normal disc galaxies. For example, H I clouds in the leading arm of the Magellanic Stream tend to be devoid of stars (Putman, Gibson & Staveley-Smith 1998). The only evidence seen in this study for such processes is the faint loop of gas seen extending outside the optical disc of ESO 381-G009 in the group CCG 1. While a conclusion of this study has been that this group is most likely to be a chance projection of three galaxies in the Centaurus cluster and not a true compact group, the members of the group will nevertheless be subject to long-term and weak gravitational effects due to the cluster potential, and the occasional high-speed encounter with other cluster members. Either of these effects can explain the gas loop, as well as provide a mechanism to trigger the ongoing star formation in the southern group member ESO 381-G008.

Finally, it is noteworthy that Xu, Sulentic & Tuffs (1999) have recently discovered a starburst region embedded in the intragroup gas in Stephan's Quintet, and believe it to be the result of a high velocity ($\sim 1000 \, km \, s^{-1}$) collision between an intruder galaxy and the cold intragroup medium. With mechanisms now established in the literature for the triggering of starbursts by mild galaxy harassment (e.g. Moore et al. 1996), by low-velocity galaxy–galaxy mergers (Jog & Solomon 1992) and by high-velocity galaxy impact on the intragroup medium itself (Xu et al. 1999), it seems likely that active star formation with a broad spectrum of triggers should be going on in physically compact groups, and to a lesser extent in loose groups. Evidence for these types of processes has already been noted in this study (viz. the possibility of galaxy harassment in CCG 1 and the likelihood of a present-day merger event in LGG 138), and in the previous work described in Section 2.3. A more thorough study of galaxy groups – perhaps based on the sample described below – is now warranted to provide real data for comparison with detailed numerical modelling of the suggested trigger mechanisms.

6.1 A future H I-selected sample of groups

One of the most promising outcomes of this study is the easy

identification of groups of galaxies in HIPASS images. The HIPASS survey has imaged extragalactic H I in the entire southern sky to a redshift of 0.04 at a velocity resolution of 18 km s^{-1}, and there are expected to be 5000–10 000 galaxies catalogued by the survey. A substantial fraction of these galaxies will be members of groups. Groups selected from the HIPASS catalogue will naturally be H I-rich compared to those in previously published group catalogues, and will probably contain a higher spiral fraction than optically selected group samples. Additionally, an H I group sample will be less biased towards optically bright galaxies than are present catalogues. Therefore a simple study of the catalogue would immediately contribute to the presently unanswered question of whether galaxy groups are deficient in spiral galaxies.

The Hickson (1982) criteria accept compact groups only where four galaxies are within three magnitudes of the brightest. It is likely that this selection is partly responsible for the intragroup morphological concordance seen in groups (Sulentic 1987), and a full redshift–position space search, like that afforded by the HIPASS data, should reveal many more groups with member galaxies exhibiting much greater magnitude differences. The kinematics and dynamics of these 'brightness-dispersed' groups may be particularly interesting with respect to perturbations of large galaxy discs by dwarf intruders, or tidal destruction of gas-rich dwarf galaxies by compact, dark potentials.

ACKNOWLEDGMENTS

The Australia Telescope and the Parkes 64-m radiotelescope are funded by the Commonwealth of Australia for operation as National Facilities managed by CSIRO. Assistance with observing from M. Brown, D. Mortlock and C. Fluke was greatly appreciated. We thank L. Staveley-Smith, F. Briggs and S. Schneider for their many valuable comments which improved this study. The Multibeam Survey Working Group is thanked for providing HIPASS data in advance of its publication.

REFERENCES

Agüero E. L., Calderón J. H., Paolantonio S., Suárez Boedo E., 1994, PASP, 106, 978
Allam S., Assendorp R., Longo G., Braun M., Richter G., 1996, A&AS, 117, 39
Allen C. W., 1973, Astrophysical Quantities. Athlone Press, London
Arp H. C., Madore B. F., 1987, A Catalogue of Southern Peculiar Galaxies and Associations. Cambridge Univ. Press, Cambridge
Barnes D. G., 1998, PhD thesis, Univ. Melbourne
Barnes D. G., 1999, Publ. Astron. Soc. Aust., 16, 77
Barnes D. G., Drinkwater M. J., 1994, in Chapman J., Cannon R., Harrison S., Hidayat B., eds, ASP Conf. Ser. Vol. 84, The Future Utilisation of Schmidt Telescopes. Astron. Soc. Pac., San Francisco, p. 490
Barnes D. G. et al., 2001, MNRAS, 322, 486
Bettoni D., Galletta G., 1997, A&AS, 124, 61
Bottinelli L., Durand N., Fouqué P., Garnier R., Gouguenheim L., Paturel G., Teerikorpi P., 1992, A&AS, 93, 173
Bottinelli L. et al., 1993, A&AS, 102, 57
Chengalur J. N., Salpeter E. E., Terzian Y., 1993, ApJ, 419, 30
Clark B. G., 1980, A&A, 89, 377
Corwin H. G., de Vaucouleurs A., de Vaucouleurs G., 1985, Southern Galaxy Catalogue of Bright Galaxies. Univ. Texas Monographs in Astronomy
da Costa L. N., Pellegrini P. S., Davis M., Meiksin A., Sargent W. L. W., Tonry J. L., 1991, ApJS, 75, 935
de Grijp M. H. K., Miley G. K., Lub J., 1987, A&AS, 70, 95
de Vaucouleurs G., Corwin H. G., de Vaucouleurs A. P., 1976, Second Reference Catalogue of Bright Galaxies. Univ. Texas Press, Austin
de Vaucouleurs G., de Vaucouleurs A. P., Corwin H. G., Buta R., Paturel G., Fouqué P., 1991, Third Reference Catalogue of Bright Galaxies. Springer-Verlag, New York
Ebeling H., Voges W., Böringer H., 1994, ApJ, 436, 44
Ferguson H. C., Sandage A., 1990, AJ, 100, 1
Fouqué P., Gourgoulhon E., Chamaraux P., Paturel G., 1992, A&AS, 93, 211
Garcia A. M., 1993, A&AS, 100, 47
Garcia A. M., 1995, A&A, 297, 56
Garcia A. M., Bottinelli L., Durand N., Garnier R., Gouguenheim L., Paturel G., 1994, A&AS, 107, 265
Gonzalez Delgado R. M., Perez E., Tadhunter C., Vilchez J. M., Rodriguez-Espinosa J. M., 1997, ApJS, 108, 155
Gourgoulhon E., Chamaraux P., Fouqué P., 1992, A&A, 255, 69
Heisler J., Tremaine S., Bahcall J. N., 1985, ApJ, 298, 8
Hickson P., 1982, ApJ, 255, 382
Hickson P., 1997, ARA&A, 35, 357
Hickson P., Rood H. J., 1988, ApJ, 331, L69
Hickson P., Mendes de Oliveira C., Huchra J. P., Palumbo G. G. C., 1992, ApJ, 399, 353
Higdon J. L., 1996, ApJ, 467, 241
Hopp U., Materne J., 1985, A&AS, 61, 93
Huchtmeier W. K., Richter O.-G., 1989, A General Catalog of H I Observations of Galaxies. Springer-Verlag, New York
Jog C. J., Solomon P. M., 1992, ApJ, 387, 152
Jörsäter S., van Moorsel G. A., 1995, AJ, 110, 2037
Keel W. C., 1996a, ApJS, 106, 27
Keel W. C., 1996b, AJ, 111, 696
Kennicutt R. C., 1989, ApJ, 344, 685
Koribalski B., 1996, in Skillman E., eds, ASP Conf. Ser. Vol. 106, The Minnesota Lectures on Extragalactic H I. Astron. Soc. Pac., San Francisco, p. 238
Lauberts A., 1982, The ESO/Uppsala Survey of the ESO(B) Atlas. European Southern Observatory
Lauberts A., Valentijn E., 1989, The Surface Photometry Catalogue of the ESO-Uppsala Galaxies. European Southern Observatory
Ledlow M. J., Loken C., Burns J. O., Hill J. M., White R. A., 1996, AJ, 112, 388
Malin D., Hadley B., 1997, PASA, 14, 52
Mathewson D. S., Ford V. L., 1996, ApJS, 107, 97
Mendes de Oliveira C., 1995, MNRAS, 273, 139
Moore B., Katz N., Lake G., Dressler A., Oemler A., Jr, 1996, Nat, 379, 613
Nolthenius R., 1993, ApJS, 85, 1
Oosterloo T., Iovino A., 1997, PASA, 14, 48
Pildis R. A., Bregman J. N., Evrard A. E., 1995, ApJ, 443, 514
Pildis R. A., Evrard A. E., Bregman J. N., 1996, AJ, 112, 378
Plana H., Amram P., Mendes de Oliveira C., Balkowski C., 2000, AJ, 120, 621
Ponman T. J., Bertram D., 1993, Nat, 363, 51
Prandoni I., Iovino A., MacGillivray H. T., 1994, AJ, 107, 1235
Putman M. E., Gibson B. K., Staveley-Smith L., 1998, in Chu Y.-H., Suntzeff B., Hesser J. E., Bohlender D. A., eds, Proc. IAU Symp. 190, New Views of the Magellanic Clouds. Astron. Soc. Pac., San Francisco, p. 51
Ramella M., Diaferio A., Geller M. J., Huchra J. P., 1994, AJ, 107, 1623
Reynolds J., 1994, A Revised Flux Scale for the AT Compact Array. ATNF Internal Report, AT/39.3/040
Ribeiro A. L. B., de Carvalho R., Coziol R., Capelato H. V., Zepf S. E., 1996, ApJ, 463, L5
Roberts M. S., Haynes M. P., 1994, ARA&A, 32, 115
Rood H. J., Struble M. F., 1994, PASP, 106, 413
Rose J. A., 1977, ApJ, 211, 311
Rubin V. C., Ford W. K., Jr, Hunter D. A., 1990, ApJ, 365, 86
Rubin V. C., Ford W. K., Jr, Hunter D. A., 1991, ApJS, 76, 153
Sanders D. B., Mirabel I. F., 1996, ARA&A, 34, 749

Shostak G. S., Sullivan W. T., Allen R. J., 1984, A&A, 139, 15
Strauss M. A., Huchra J. P., Davis M., Yahil A., Fisher K. B., Tonry J., 1992, ApJS, 83, 29
Sulentic J. W., 1987, ApJ, 322, 605
Takata T., Yamada T., Saito M., Chamaraux P., Kazes I., 1994, A&AS, 104, 529
Tully R. B., 1987, ApJ, 321, 280
Vorontsov-Velyaminov B. A., 1977, A&AS, 28, 1
Walke D. G., Mamon G. A., 1989, A&A, 225, 291
Williams B. A., Rood H. J., 1987, ApJS, 63, 265
Williams B. A., van Gorkom J. H., 1988, AJ, 95, 352
Williams B. A., McMahon P. M., van Gorkom J. H., 1991, AJ, 101, 1957
Xu C., Sulentic J. W., Tuffs R., 1999, ApJ, 512, 178
Yamada T., Tomita A., Saito M., Chamaraux P., Kazes I., 1994, MNRAS, 270, 93
Zepf S. E., 1993, ApJ, 407, 448

This paper has been typeset from a TEX/LATEX file prepared by the author.